Journal of Molecular Structure 1110 (2016) 102–113

Contents lists available at ScienceDirect

Journal of Molecular Structure

journal homepage: http://www.elsevier.com/locate/molstruc

Novel 2-amino-1,3,4-thiadiazoles and their acyl derivatives: Synthesis, structural characterization, molecular docking studies and comparison of experimental and computational results

Mustafa Er [a, *], Gamze Isildak [b], Hakan Tahtaci [c], Tuncay Karakurt [d]

[a] Department of Chemical Engineering, Faculty of Engineering, Karabuk University, 78050 Karabuk, Turkey
[b] Department of Chemistry, Faculty of Science, Karabuk University, 78050 Karabuk, Turkey
[c] Department of Polymer Engineering, Faculty of Technology, Karabuk University, 78050 Karabuk, Turkey
[d] Department of Chemical Engineering, Faculty of Engineering and Architecture, Ahi Evran University, 40100, Kırşehir, Turkey

ARTICLE INFO

Article history:
Received 1 September 2015
Received in revised form
17 January 2016
Accepted 18 January 2016
Available online 20 January 2016

Keywords:
2-amino-1,3,4-thiadiazole
Crystal structure
NMR
B3LYP

ABSTRACT

This study aims to synthesize and characterize compounds containing 2-amino-1,3,4-thiadiazole and compare experimental results to theoretical results. For this purpose, firstly mono, di and tetra 2-amino-1,3,4-thiadiazole compounds **(2a–c, 14, 20 and 25)** were synthesized in relatively high yields (74–87%). The target compounds **(3–11**, **15–17**, **21–23** and **26–28)** were then synthesized in moderate to high yields (65–85%) from the reactions of 2-amino-1,3,4-thiadiazole compounds with various acyl chloride derivatives.

The structures of all synthesized compounds were elucidated by IR, ^{1}H NMR, ^{13}C NMR, elemental analyses and mass spectroscopy techniques. The structures of **2b** ($C_9H_8N_4O_2S$) and **2c** ($C_{11}H_{13}N_3O_2S$) were also elucidated by X-ray diffraction analysis.

Lastly, IR spectrum, ^{1}H NMR and ^{13}C NMR chemical shift values, frontier molecular orbital (FMO) values of these molecules containing heteroatoms were examined using the Becke-3- Lee-Yang-Parr (B3LYP) method with the 6-31G(d) basis set. Two different molecular structures containing 2-amino-1,3,4-thiadiazole **(2b, 2c)** were used in our study to examine these properties. Also, compounds **2b** and **2c** form a stable complex with beta-Lactamase as can be understood from the binding affinity values and the results show that the compound might inhibit the beta-Lactamase enzyme. It was found that theoretical and experimental results obtained in the experiment were compatible with each other and with the values found in the literature.

1. Introduction

In recent years, despite significant increases in their discovery, the uses of compounds with biological activities were quite limited due to the development of resistance against these compounds and the presence of various side effects. For these reasons, chemists have been striving to develop compounds with biological activities for use in pharmaceutical chemistry.

Thiadiazole is a five-membered heterocyclic aromatic compound with the molecular formula of $C_2H_2N_2S$. 1,3,4-Thiadiazole and its derivatives have become the focus of attention in drug, agriculture and material chemistry due to their high activity in 2′ and 5′ positions against nucleophilic substitution reactions [1–8]. The –N=C–S group in the structure allows for great structural stability and is known to be the component responsible for biological activity [9,10]. 1,3,4-thiadiazole and its heterocyclic derivatives have been synthesized on a large scale for many years due to a variety of biological activities, including antifungal, antibacterial, antimicrobial, anti-inflammatory, anticonvulsant, anti-HIV, antituberculosis, and antiproliferative activities [11–27]. The synthesis of these compounds is particularly important due to the high anticancer activities of 2-amino-1,3,4-thiadiazole and derivatives, [28–31]. In addition, it has been reported in various studies conducted with 1,3,4-thiadiazole and its derivatives that these compounds were used in various areas such as polymer, dye, herbicide

* Corresponding author. Tel.: +90 370 4332021; fax: +90 370 4333290.
E-mail addresses: mustafaer@karabuk.edu.tr (M. Er), isildak.g@hotmail.com (G. Isildak), hakantahtaci@karabuk.edu.tr (H. Tahtaci), tuncaykarakurt@gmail.com (T. Karakurt).

http://dx.doi.org/10.1016/j.molstruc.2016.01.045
0022-2860/

and insecticide production [32–35].

Today, beta-lactam antibiotics are the most widely used antibiotic derivatives. The most important source of resistance against beta-lactam antibiotic derivatives for members of *Enterobacteriaceae* are beta-lactamase enzymes secreted by bacteria. Beta-lactamase enzymes are mostly synthesized by Gram negative bacteria and cause resistance against antibiotics that carry beta-lactam ring [36]. Beta-lactam antibiotics inhibit transpeptidase and carboxypeptidase enzymes, which are responsible for peptidoglycan synthesis, and inhibit cell wall synthesis [37]. The most significant pathogen that synthesizes beta-lactamase among Gram-positive bacteria is *Staphylococcus aureus*.

In the light of the important data gathered through research of the literature, the primary purpose of this study was to synthesize a variety of substituted groups containing 1,3,4-thiadiazole ring with potential biological activity, acylate these compounds with various acyl groups, and to characterize them. The synthetic routes of all synthesized compounds are given in Schemes 1–4.

The secondary purpose of the study was to theoretically examine the following properties of the synthesized compounds to support experimental studies: IR, NMR spectra and frontier molecular orbital (FMO).

Also, structures of **2b** and **2c** compounds were compared with the ligands of prominent antibacterial targets in terms of similarity. Trial docking studies made for this enzyme showed that the crystal structure 1BLH of beta-Lactamase from *S. aureus* was the most appropriate target of the **2b** and **2c** compounds.

2. Experimental

2.1. Materials and methods

The reactions were carried out under a nitrogen atmosphere using standard Schlenk techniques. The ^{1}H NMR and ^{13}C NMR spectra of the compounds were recorded in DMSO-d_6 using an Agilent NMR VNMRS spectrometer at 400 MHz and 100 MHz, respectively. TMS was used as an internal standard. The IR spectra were measured in ATR using a Perkin Elmer FT-IR Spectrometer Frontier. The mass spectra were measured with a Thermo TSQ Quantum Access Max LC-MS/MS spectrometer. Elemental analyses were performed on a LECO 932 CHNS (Leco-932, St. Joseph, MI, USA) instrument and the results were within ±0.4% of the theoretical values. Melting points were recorded on a Thermo Scientific IA9000 series apparatus and were uncorrected. All of the chemicals were obtained from Merck Chemicals.

2.2. Synthesis

2.2.1. General method for the synthesis of mono 2-amino-1,3,4-thiadiazole derivatives (**2a–c**)

In a round-bottomed flask, compounds **(1a–c)** (0.002 mol) and thiosemicarbazide (0.003 mol) in trifluoroacetic acid (5 mL) at 60 °C were stirred for 3–5 h. The progress of the reaction was monitored by TLC at appropriate time intervals. After completion of the reaction, the mixture was poured into 200 mL of ice-cold water and neutralized with ammonia. The solution was filtered and the solid matter was obtained. It was washed with deionized water, ethanol and diethyl ether, respectively. The solid was recrystallized from the appropriate solvent. The physical properties and spectral data derived from the obtained products are listed below.

2.2.1.1. 5-(thiophen-2-ylmethyl)-1,3,4-thiadiazol-2-amine ***(2a)***. Yield: (74%); White solid, mp 183–184 °C (from DMF-EtOH, 1:3). IR (ATR, cm^{-1}): 3260–3100 ($-NH_2$), 3045 (Ar-CH), 2973 (Aliph. CH), 1517–1503 (C=N), 1159 (N–N), 622–578 (C–S). ^{1}H NMR (400 MHz, DMSO-d_6) δ (ppm): 4.36 (s, 2H, $-CH_2$), Thiophene-H [6.93 (d,

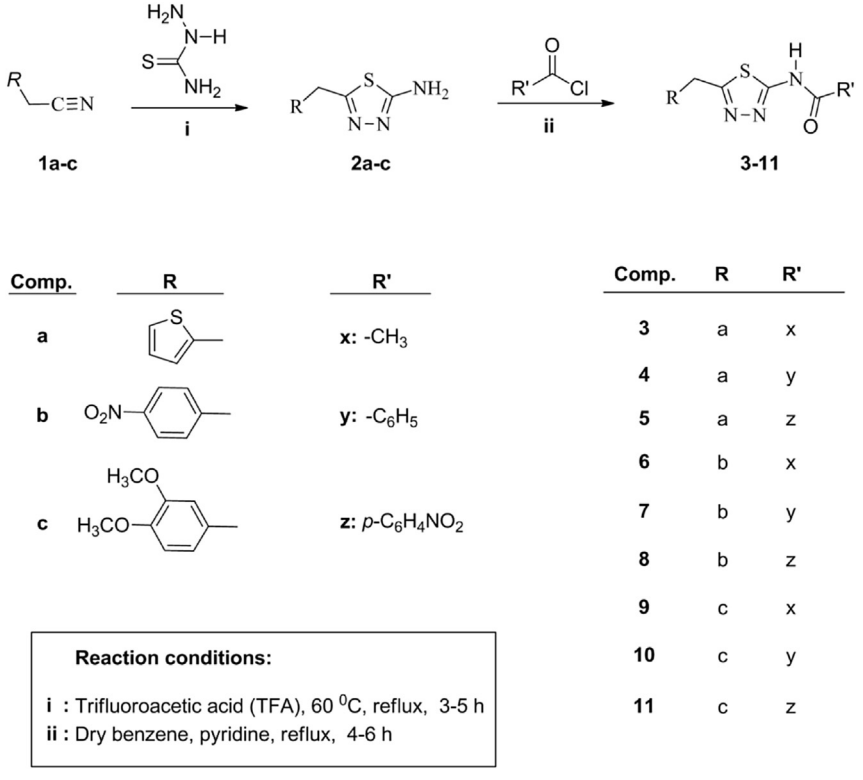

Scheme 1. General synthesis of mono 2-amino-1,3,4-thiadiazole derivatives (**2a–c**), and their acyl derivatives (**3–11**).

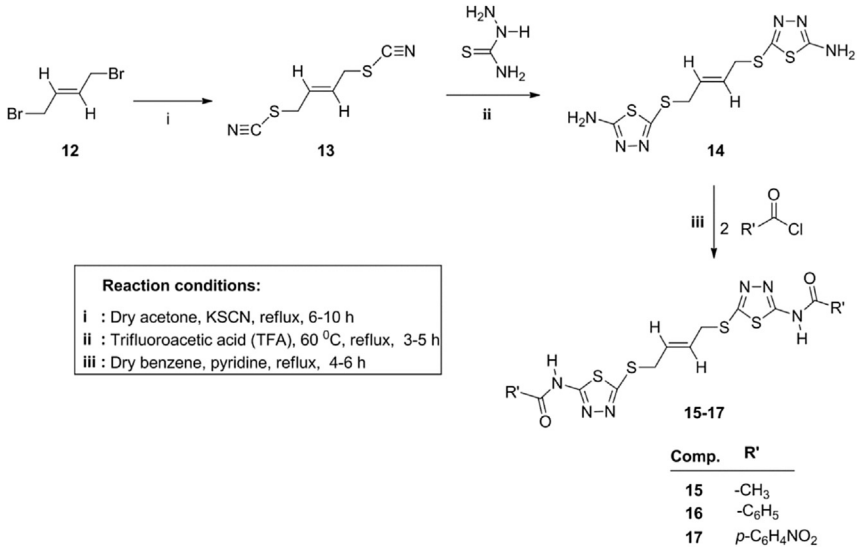

Scheme 2. General synthesis of di 2-amino-1,3,4-thiadiazole derivative (**14**), and its acyl derivatives (**15**–**17**).

$J = 5.2$ Hz, 1H), 6.96 (d, $J = 5.2$ Hz, 1H), 7.38 (dd, $J = 5.2$, 2.8 Hz, 1H)], 7.10 (s, 2H, NH_2). ^{13}C NMR (100 MHz, DMSO-d_6, δ ppm): 30.54 ($-CH_2$), Thiophene-C [126.12 (CH), 127.01 (CH), 127.80 (CH), 140.71 (C)], Thiadiazole-C [157.71 (C), 169.71 (C)]. Analysis (% calculated/found) for $C_7H_7S_2N_3$ (Mw 197.28) C: 42.62/42.69; H: 3.58/3.67; N:21.30/21.33. MS (ESI-*m/z*): 198.02 (M + 1, 100).

2.2.1.2. 5-(4-nitrobenzyl)-1,3,4-thiadiazol-2-amine ***(2b)***. Yield: (75%); White crystals, mp 181–182 °C (from DMF-EtOH, 1:3). IR (ATR, cm^{-1}): 3271–3112 ($-NH_2$), 3067 (Ar-CH), 2954 (Aliph. CH), 1531–1506 (C=N), 1155 (N–N), 622–603 (C–S). ^1H NMR (400 MHz, DMSO-d_6) δ (ppm): 4.32 (s, 2H, $-CH_2$), Phenyl-H [7.54 (d, $J = 8.0$ Hz, 2H), (8.16 (d, $J = 8.0$ Hz, 2H)], 7.14 (s, 2H, NH_2). ^{13}C NMR (100 MHz, DMSO-d_6, δ ppm): 35.59 ($-CH_2$), Phenyl-C [124.42 (CH), 130.67 (CH), 146.54 (C), 147.08 (C)], Thiadiazole-C [156.39 (C), 169.78 (C)]. Analysis (% calculated/found) for $C_9H_8N_4O_2S$ (Mw 236.25) C: 45.75/45.59; H: 3.41/3.45; N:23.72/23.78. MS (ESI-*m/z*): 237.06 (M + 1, 100).

2.2.1.3. 5-(3,4-dimethoxybenzyl)-1,3,4-thiadiazol-2-amine ***(2c)***. Yield: (87%); White crystals, mp 205–207 °C (from DMF-EtOH, 1:3). IR (ATR, cm^{-1}): 3267–3083 ($-NH_2$), 3028 (Ar-CH), 2959 (Aliph. CH), 1589–1511 (C=N), 1135 (N–N), 633–577 (C–S). ^1H NMR (400 MHz, DMSO-d_6) δ (ppm): 3.71 (s, 6H, OCH_3), 4.04 (s, 2H, $-CH_2$), Phenyl-H [6.75 (d, $J = 7.2$ Hz, 1H), 6.85 (s, 1H), 6.87 (d, $J = 7.2$ Hz, 1H)], 7.02 (s, 2H, NH_2). ^{13}C NMR (100 MHz, DMSO-d_6, δ ppm): 35.83 ($-CH_2$), 56.08 ($-OCH_3$), Phenyl-C [112.53 (CH), 112.95 (CH), 121.27 (CH), 131.06 (C), 148.34 (C), 149.37 (C)], Thiadiazole-C [159.03 (C), 169.46 (C)]. Analysis (% calculated/found) for $C_{11}H_{13}N_3O_2S$ (Mw 251.30) C: 52.57/52.59; H: 5.21/5.25; N:16.72/16.78. MS (ESI-*m/z*): 274.08 (M + Na, 100).

2.2.2. General acylation reactions of mono 2-amino-1,3,4-thiadiazole derivatives ***(3–11)***

In a two-necked flask, compounds **(2a–c)** (0.003 mol) were suspended in dry benzene (40 mL) and pyridine (1 mL). Acyl chloride derivatives (0.003 mol) were added drop-wise to this

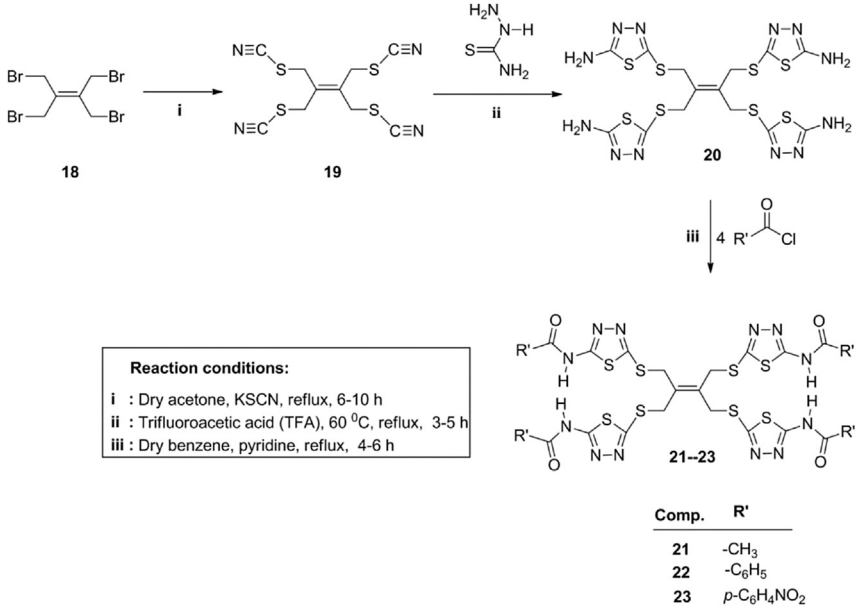

Scheme 3. General synthesis of tetra 2-amino-1,3,4-thiadiazole derivative (**20**), and its acyl derivatives (**21**–**23**).

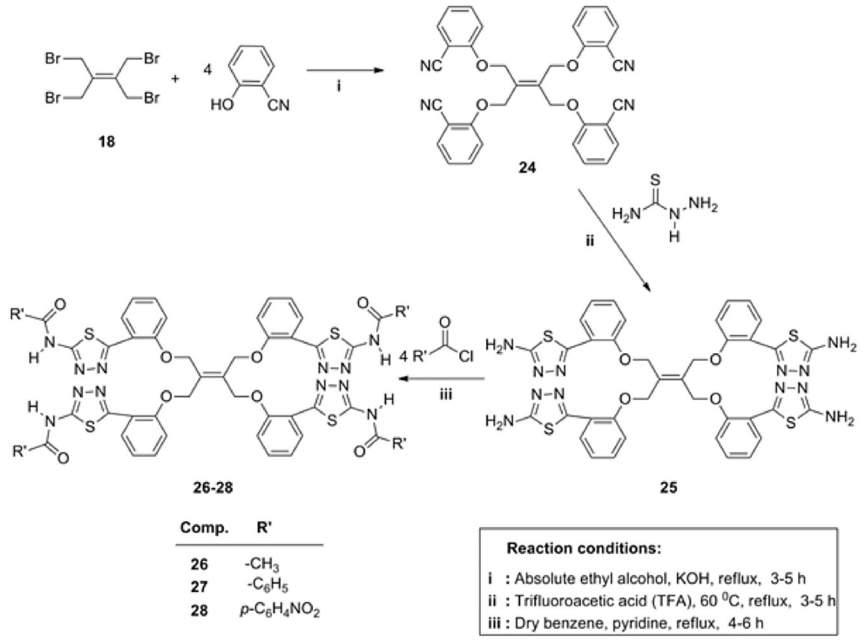

Scheme 4. General synthesis of tetra oxy 2-amino-1,3,4-thiazdiazole derivative (**25**), and its acyl derivatives (**26**–**28**).

solution at room temperature with the assistance of a dropping funnel. The mixture was then refluxed and stirred for 4–6 h. The progress of the reaction was monitored by TLC at appropriate time intervals. After completion of the reaction, the solution was filtered and the solid matter was obtained. It was washed with deionized water, ethanol and diethyl ether, respectively. The solid matter was recrystallized from the appropriate solvent. All physical properties and spectral data derived from the obtained products are given in the Supplementary Material Section.

*2.2.3. General acylation reactions of di 2-amino-1,3,4-thiadiazole derivatives **(15–17)***

In a two-necked flask, compound **(14)** (0.003 mol) was suspended in dry benzene (40 mL) and pyridine (1 mL). Acyl chloride derivatives (0.006 mol) were added drop-wise to this solution at room temperature with the assistance of a dropping funnel. The mixture was then refluxed and stirred for 4–6 h. The progress of the reaction was monitored by TLC at appropriate time intervals. After completion of the reaction, the solution was filtered and the solid matter was obtained. It was washed with deionized water, ethanol and diethyl ether, respectively. The solid matter was recrystallized from the appropriate solvent. All physical properties and spectral data derived from the obtained products are given in the Supplementary Material Section.

*2.2.4. General acylation reactions of tetra 2-amino-1,3,4-thiadiazole derivatives **(21–23)***

In a two-necked flask, compound **(20)** (0.003 mol) was suspended in dry benzene (40 mL) and pyridine (1 mL). Acyl chloride derivatives (0.012 mol) were added drop-wise to this solution at room temperature with the assistance of a dropping funnel. The mixture was then refluxed and stirred for 4–6 h. The progress of the reaction was monitored by TLC at appropriate time intervals. After completion of the reaction, the solution was filtered and the solid matter was obtained. It was washed with deionized water, ethanol and diethyl ether, respectively. The solid matter was recrystallized from the appropriate solvent. All physical properties and spectral data derived from the obtained products are given in the Supplementary Material Section.

*2.2.5. General acylation reactions of tetra oxy 2-amino-1,3,4-thiadiazole derivatives **(26–28)***

In a two-necked flask, compound **(25)** (0.003 mol) was suspended in dry benzene (40 mL) and pyridine (1 mL). Acyl chloride derivatives (0.012 mol) were added drop-wise to this solution at room temperature with the assistance of a dropping funnel. The mixture was then refluxed and stirred for 4–6 h. The progress of the reaction was monitored by TLC at appropriate time intervals. After completion of the reaction, the solution was filtered and the solid matter was obtained. It was washed with deionized water, ethanol and diethyl ether, respectively. The solid matter was recrystallized from the appropriate solvent. All physical properties and spectral data derived from the obtained products are given in the Supplementary Material Section.

3. X-ray crystal structure determination and theoretical calculations

X-ray diffraction data of the crystals was collected with a Bruker AXS APEX CCD [38] diffractometer and a MoKα beam. The structure solution of the crystals was performed with the SHELXT-2014 [39] program using direct methods. In order to determine the positions of atoms other than hydrogen in the solution phase, the refinement process was performed with the SHELXL-2014 [39] program which depends on the full-matrix least-squares method. Isotropic refinement was used in the first phase in order to increase the sensitivity of the atom positions and determine the missing atoms. No missing atoms were discovered other than hydrogen. This data was seen as a result of the refinement process and anisotropic refinement was then performed. Hydrogen atoms were determined in the following phase of the refinement. The positions of hydrogen atoms were obtained geometrically using the overlapping method. When placing hydrogen atoms geometrically, aromatic bond lengths were fixed at the following positions: 0.93 Å, methylene ($-CH_2$) bond lengths at 0.97 Å; methyl ($-CH_3$) bond lengths at 0.96 Å; and N–H bond lengths at 0.86 Å. After the structure solution

and refinement processes, the ORTEP-3 [40] program was used for molecular drawings and PLATON [41], WinGX [40], and MERCURY [42] programs were used for calculations. Theoretical calculations related to the compounds were performed with the 6-31G(d) basis set [43], the DFT(B3LYP) [44] theory, the Gaussian09 program [45], and the Gausview 5 program [46] which was used to examine Gaussian outputs graphically.

4. Results and discussion

In the first part of the study, 2-amino-1,3,4-thiadiazole derivatives **(2a–c, 14, 20,** and **25)** were synthesized in high yields (74–87%) from the reaction of nitrile compounds **(1a–c, 13, 19,** and **24)** with thiosemicarbazide in trifluoroacetic acid (TFA) at 60 °C. Nitrile derivatives used as initial compounds **(1a–c)** were obtained by purchase, while nitrile compounds **(13**, **19,** and **24)** were obtained as specified in the literature [47,48].

Compelling data from the experiment includes the fact that sharp absorption bands belonging to the –C≡N group observed in the range of 2220–2269 cm^{-1} in nitrile derivatives in IR spectrum disappeared, and symmetric and asymmetric absorption bands corresponding to the $-NH_2$ group in 2-amino-1,3,4-thiadiazole derivatives emerged as two separate bands in the range of 3296–3112 cm^{-1}. This data provides the most important evidence for cyclization.

The structures of 2-amino-1,3,4-thiadiazole derivatives **(2a–c, 14, 20, and 25)** were also confirmed by the assistance of ^1H NMR spectroscopy.

The $-NH_2$ group proton signals of compounds **2a–c** bonded to 1,3,4-thiadiazole ring from C-2 position in ^1H NMR spectra were recorded as a singlet corresponding to two protons in the range of 7.14–7.02 ppm. Proton peaks belonging to the $-NH_2$ group disappeared as a result of the proton–deuterium exchange performed with D_2O. The methylene ($-CH_2$) protons bonding thiophene and phenyl groups to the thiadiazole ring from the 5-position were observed as a singlet corresponding to two protons in the range of 4.36–4.04 ppm. Proton peaks belonging to the thiophene ring were determined as a doublet corresponding to one proton at 6.93 and 6.96 ppm and as a doublet of a doublet corresponding to one proton at 7.38 ppm.

In compound **14**, the $-NH_2$ proton signal at the 2-position of the thiadiazole ring was observed as a singlet corresponding to four protons at 7.31 ppm. In compounds **20** and **25**, tetra analogs of compound **14**, the proton signal was observed as a singlet corresponding to eight protons at 7.37 ppm and 7.14 ppm, respectively. In compound **14**, methylene protons ($-S-CH_2$) were observed as a singlet corresponding to four protons at 3.69 ppm, while in compound **20**, these peaks were determined to be a singlet corresponding to eight protons at 3.88 ppm. In compound **25**, the methylene protons ($-O-CH_2$) bonded to the aromatic ring were observed as a singlet corresponding to eight protons at 5.21 ppm in the low field due to electronegativity of the oxygen atom. Vinylic (–CH=CH) protons in the compound **14** were observed as a broad singlet at 5.76 ppm. Singlet peaks observed at 7.14 ppm, 7.31 ppm, and 7.37 ppm disappeared almost entirely and supported the suggested structures, especially in exchange treatments of the $-NH_2$ groups bonded to the 2-position of thiadiazole in these compounds with D_2O. Other ^1H NMR spectra results of these structures are given in detail in the Supplementary Material Section.

The structures of 2-amino-1,3,4-thiadiazole derivatives **(2a–c, 14, 20, and 25)** were also confirmed by the assistance of ^{13}C NMR spectroscopy. In ^{13}C NMR spectra, it was observed that resonance values of carbons at C-2 and C-5 positions of the 2-amino-1,3,4-thiadiazole ring were highly compatible with these types of compounds in the literature [49].

C-2 carbon signals of the 2-amino-1,3,4-thiadiazole ring in these compounds were recorded in the range of 159.03–148.35 ppm and C-5 carbon signals were recorded in the range of 170.19–169.46 ppm. In addition, sp^3 hybridized methylene group ($-S-CH_2$) carbons appeared in compounds **14** and **20** at 35.77 ppm and 35.52 ppm, respectively. Methylene group ($-OCH_2$) carbons in the compound **25** appeared at 65.16 ppm due to the electronegativity of the oxygen atom. sp^3 hybridized methylene group ($-CH_2$) carbon signals in the **2a–c** compounds were recorded in the range of 35.83–30.57 ppm. While sp^3 hybridized vinyl group (–CH=CH) carbons in compound **14** were observed at 128.96 ppm, C=C carbon peaks in compounds **20** and **25** were observed at 133.39 and 135.13 ppm, respectively. The data belonging to the 2-amino-1,3,4-thiadiazole ring is highly compatible with the data found in the literature [50]. Other spectral data belonging to the carbon skeleton of the molecule fully supports the suggested structures. In the mass spectra belonging to these compounds, it was observed that molecular ion peaks appeared to be compatible with the suggested structures and they supported the structures.

In the second part of the study, compounds **3–11**, **15–17**, **21–23,** and **26–28** were synthesized in moderate to high yields (65–85%) from the reactions of acyl chloride derivatives with 2-amino-1,3,4-thiadiazole derivatives **(2a–c, 14, 20, and 25)** in the presence of dry benzene.

In the IR spectra of these compounds, $-NH_2$ group symmetric and asymmetric absorption bands disappeared that were found in the initial compounds and observed in the 3296–3112 cm^{-1} range. The most significant evidence that these compounds were acylated is the fact that –NH absorption bands observed in the range of 3176–3117 cm^{-1} formed in compounds **3–11**, **15–17**, **21–23**, and **26–28.** Other important evidence is the emergence of carbonyl group (C=O) absorption bands seen in the range of 1699–1657 cm^{-1} as a result of the acylation of 2-amino-1,3,4-thiadiazole.

$-NH_2$ group proton signals observed in the range of 7.37–7.02 ppm disappeared in 2-amino-1,3,4-thiadiazole derivatives **(2a–c**, **14**, **20**, **25)** which were the initial compounds of these compounds in the ^1H NMR spectra. Instead of these signals, a singlet corresponding to one proton in the 13.36–12.41 ppm range was observed in compounds **3–11.** A singlet corresponding to two protons in the 13.42–12.52 ppm range was also observed in compounds **15–17**. A singlet corresponding to four protons in the 13.38–12.30 ppm range was observed in compounds **21–23** and **26–28**, and this data is the most important evidence that these compounds were acylated.

In addition, peaks observed in the 7.37–7.02 ppm range of the-NH_2 group in 2-amino-1,3,4-thiadiazole derivatives **(2a–c**, **14**, **20**, **25)** shifted to high ppm values after the acylation due to the electron withdrawing property of the carbonyl group. This data is considered as more important evidence regarding these structures and it is consistent with findings in the literature [51]. –NH proton signals (–NH–C=O) of resulting compounds **3–11, 15–17, 21–23** and **26–28** observed at 13.38–12.30 ppm disappeared after the exchange treatment with D_2O.

These compounds' C=O group signals belonging to the acyl group in ^{13}C NMR spectra appeared in the range of 169.57–160.36 ppm. The fact that these peaks were found in ^{13}C NMR spectrum is also considered important evidence that the amino group at the 2-position of the thiadiazole ring was acylated. Other ^{13}C NMR spectra results of these compounds are given in detail in the Supplementary Material Section.

On the other hand, mass spectra of all synthesized compounds were observed as expected and supported by molecular ion peaks. Spectra (IR, ^1H NMR, ^{13}C NMR, and mass) of all synthesized compounds are given in the Supplementary Material Section.

Table 1
Crystallographic data for compounds **2b** and **2c**.

Empirical formula	$C_9H_8N_4O_2S$ **(2b)**	$C_{11}H_{13}N_3O_2S$ **(2c)**
Formula weight	236.25 (a.k.b)	251.30 (a.k.b)
Temperature	296 K	296 K
Wavelength (Å)	MoK_α, 0,71073 Å	MoK_α, 0,71073 Å
Crystal system	Monoclinic	Monoclinic
Space group	P2(1)/c	P2(1)/c
A	5.9071(5) Å	37.1645(34)
B	5.3662(5) Å	6.0621(5)
C	32.3060(3) Å	10.8956(10)
α (°)	90°	90°
β (°)	94.703(3) °	92.482(3) °
γ (°)	90°	90°
Volume	1020.61(16) $Å^3$	2452.42(5) $Å^3$
Z (molecule/cell)	4	8
Calculated density	1.54 gr cm^{-3}	1.36 gr cm^{-3}
μ	0.307 mm^{-1}	0.258 mm^{-1}
F(000)	488	1056
Crystal size(mm)	0.14 × 0.14 × 0.20	0.12 × 0.16 × 0.22
θ range	3.28°–28.32°	3.29°–27.56°
Index ranges	$-7 \leq h \leq 7, -7 \leq k \leq 7, -42 \leq l \leq 42$	$-47 \leq h \leq 49, -8 \leq k \leq 8, -14 \leq l \leq 14$
Reflections collected	29614	55145
Reflections observed [$I \geq 2\sigma(I)$]	2383	4551
Independent reflections	2521	6064
T_{min},T_{max}	0.5863, 0.7457	0.6079, 0.7457
R_{int}	0.0487	0.0656
S	1.212	1.148
R, wR	0.0540, 0.111	0.072, 0.173
Extinction correction	SHELXL-2014	SHELXL-2014
CCDC	1416511	1416512

4.1. *X-ray structure analysis of the crystals (compounds **2b** and **2c**)*

Crystal parameters belonging to $C_9H_8N_4O_2S$ **(2b)** and $C_{11}H_{13}N_3O_2S$ **(2c)** molecules, details of data collection and the refinement processes are given in Table 1. ORTEP diagrams of the molecules drawn with 40% probability ellipsoids and diagrams of input molecules used in the Gaussian program are given in Fig. 1.

The compounds have non-planar thiadiazole and phenyl rings. Compound **2c** was formed as two identical molecules in the asymmetric unit. The dihedral angle between phenyl-thiadiazole rings was 83.11° for the **2b** molecule and 87.16° for the **2c** molecule. C–S, N–N and C–N bond lengths of both molecules seem to be shorter than corresponding single bond lengths. This data indicates a multiple bond order and it restores aromaticity to the ring. Also, the C–S bond found in the thiadiazole rings contains the carbon atom with sp^2 hybridization. These results are compatible with data found in the literature [52–56]. Experimental and calculated bond lengths and bond angles are shown in Table 2.

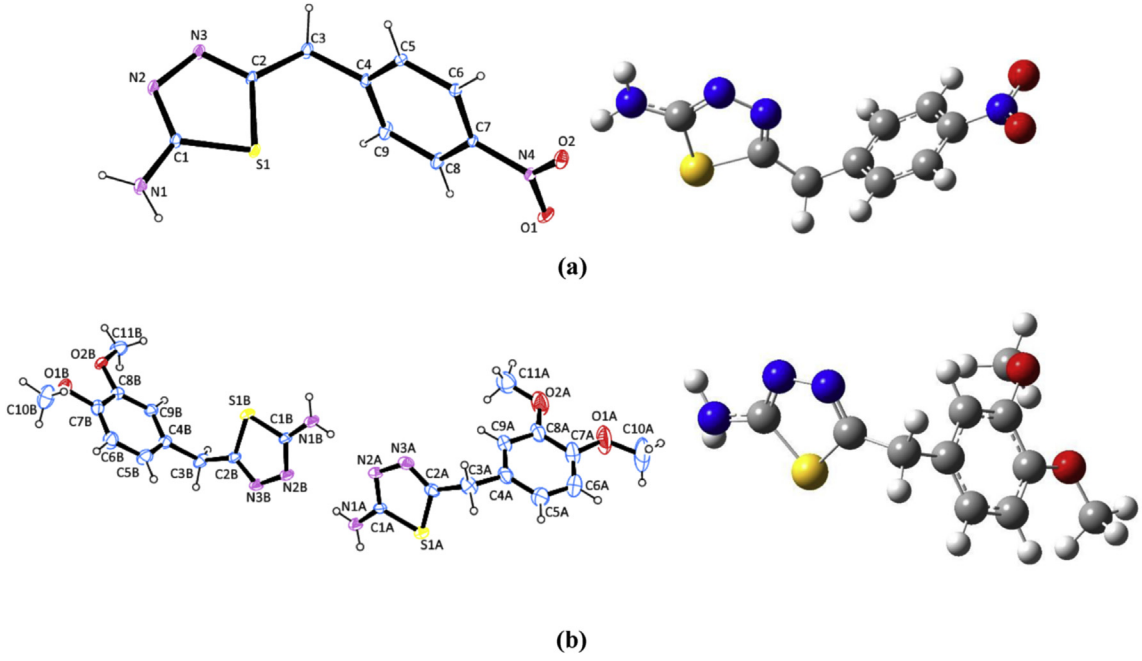

Fig. 1. (a) ORTEP-3 and calculated form of $C_9H_8N_4O_2S$ **(2b)** crystal. (b) ORTEP-3 and calculated form of $C_{11}H_{13}N_3O_2S$ **(2c)** crystal.

Table 2
Experimental and theoretical parameters belonging to compounds **2b** and **2c**.

Compound 2b ($C_9H_8N_4O_2S$)			**Compound 2c** ($C_{11}H_{13}N_3O_2S$)					
Bond length(Å)	Exp.	Cal.	Bond length(A)	Exp.	Cal.	Bond length(A)	Exp.	Cal.
S1–C1	1.732(2)	1.764	S1A–C1A	1.735(3)	1.770	S1B–C1B	1.739(3)	1.775
S1–C2	1.734(2)	1.774	S1A–C2A	1.742(3)	1.774	S1B–C2B	1.739(3)	1.775
N1–C1	1.345(3)	1.373	N2A–N3A	1.371(4)	1.371	N2B–N3B	1.385(4)	1.369
N2–N3	1.391(3)	1.370	N2A–C1A	1.310(4)	1.322	N2B–C1B	1.301(4)	1.321
N2–C1	1.308(3)	1.306	N1AA–C1A	1.283(4)	1.347	N1B–C1B	1.336(4)	1.342
N3–C2	1.283(3)	1.296	N3AA–C2A	1.339(4)	1.295	N3B–C2B	1.284(4)	1.295
C2–C3	1.507(4)	1.503	C2AA–C3A	1.493(5)	1.503	C2B–C3B	1.493(4)	1.502
Bond angles(°)			**Bond angles(°)**			**Bond angles(°)**		
C1–S1–C2	87.0(1)	84.0	C1AA–S1AA–C2A	87.6(3)	86.3	C1B–S1B–C2B	87.3(3)	86.5
S1–C2–N3	114.1(2)	112.9	SA1–C2A–N3A	112.6(3)	113.4	S1B–C2B–N3B	113.1(5)	113.1
S1–C1–N2	113.8(2)	114.3	S1A-C1A-N2A	113.2(5)	112.9	S1B–C1B–N2B	113.5(5)	112.5
N3–N2–C1	111.9(2)	113.1	N3A–N2A–C1A	112.4(5)	113.3	N3B–N2B–C1B	111.3(5)	113.4
S1–C2–C3	121.4(2)	120.5	S1A–C2A–C3A	122.3(4)	123.0	S1B–C2B–C3B	122.6(6)	123.3

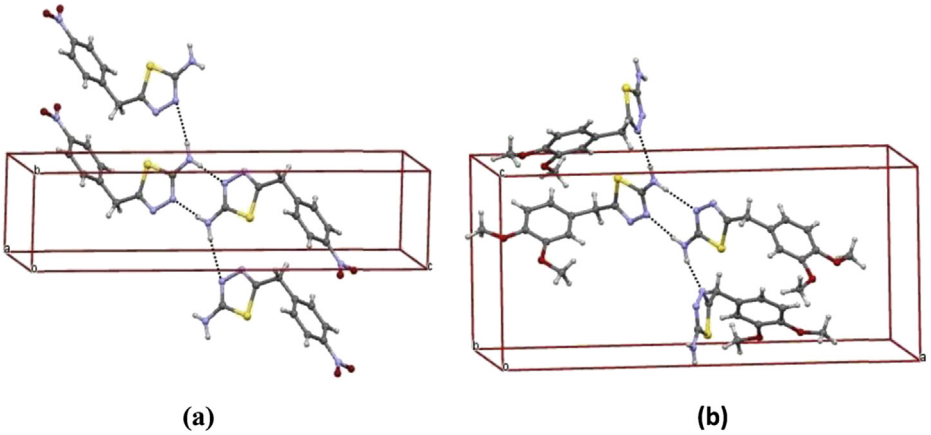

Fig. 2. Representation of intermolecular N–H···N interactions of (a) **2b**, (b) **2c** crystals.

Intermolecular N–H···N hydrogen bonds were observed in both crystals, while C–H···π interaction was observed in the **2b** molecule. The **2b** crystal is packed in three dimensional space with intermolecular N–H···N hydrogen bonds and C–H···π interactions, whereas the **2c** crystal is packed with intermolecular N–H···N hydrogen bonds. **2b** molecule formed the $R_2^2(8)$ ring motif in three dimensional space with the intermolecular hydrogen bond, which is formed by $N2^{i}$ (−x+3,−y, z) atom and H1 atom bonded to N1 atom, whereas it formed the C(9) chain with the intermolecular hydrogen bond, which is formed by $N2^{ii}$ (x, y+1, z) atom and H2 atom bonded to N1 atom (Fig. 2(a)). There is also a strong intermolecular C–H···π interaction in the structure. Intermolecular C–H···π interactions support the packing in three dimensional space. An interaction occurred between the center of the Cg1 ring identified with C1/S1/C2/N3/N2 and the H5 atom bonded to C5 atom [C5–H5···Cg^{iii}; symmetry code; (iii) −1+x,y,z] (Fig. 3). **2c** molecule formed the $R_2^2(8)$ ring motif in three dimensional space with the intermolecular hydrogen bond, which is formed by $N2A^{i}$ (x,−1+y,z) atom of the H1B atom bonded to N1B atom and $N2B^{i}$ (x,1 + y,z) atom of H1A atom bonded to N1A atom, whereas it formed the C(9) chain with the intermolecular hydrogen bond, which is formed by $N3A^{i}$ (x,5/2-y,-1/2 + z) atom of H2A atom bonded to N1A atom and $N3B^{i}$ (x,3/2−y,1/2 + z) atom of H2B atom bonded to N1B atom (Figs. 2(b) and 4).

Molecules were bound to each other with these interactions. It was observed that N–H···N hydrogen bonds formed the closed rings according to the center of symmetry. Figs. 2–4 provide diagrams of the Mercury shape belonging to the structure found as a result of the solution phase and drawings of molecules' packing in unit cells, respectively. Information related to hydrogen bonds is given in Table 3.

In theoretical calculations related to **2b** and **2c** molecules, coordinates obtained from X-ray data were used as the initial geometry. Geometric optimizations of the system were obtained using the DFT/B3LYP method and the 6-31G(d) basis set. Bond

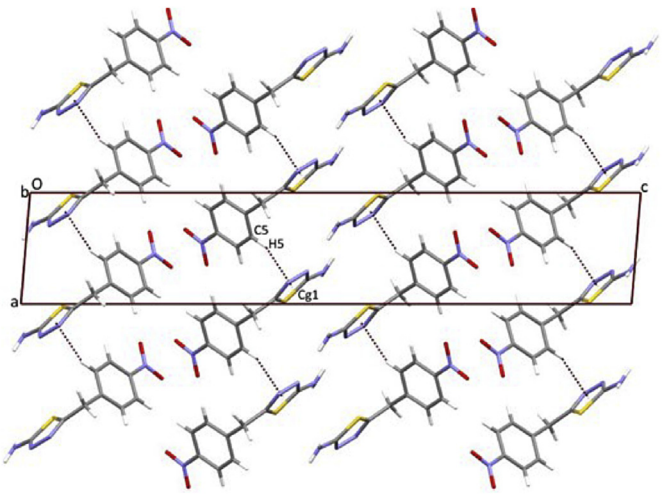

Fig. 3. Packing of the **2b** crystal with C–H···π interactions.

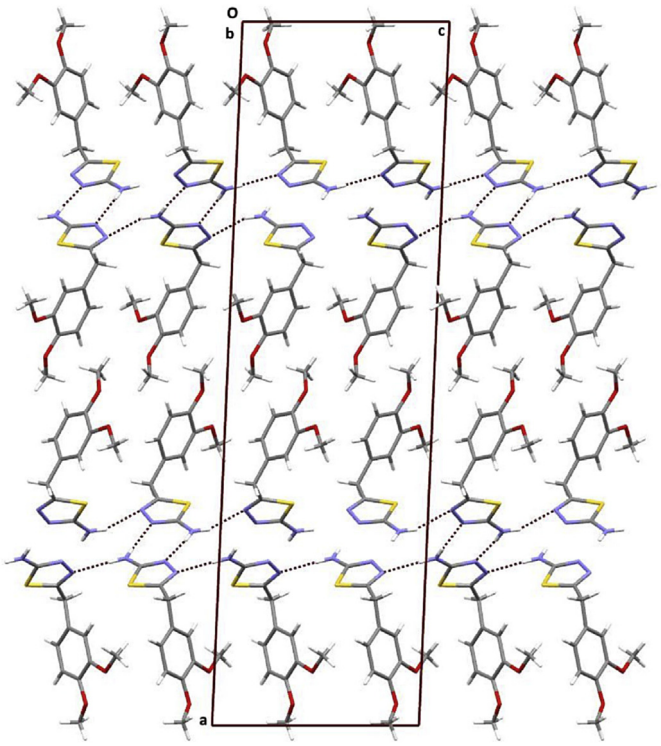

Fig. 4. Packing of the 2c crystal with N–H···N interactions.

lengths and bond angles found as a result of experimental and theoretical studies are shown in Table 2 comparatively.

4.2. IR spectra (compounds *2b* and *2c*)

While the **2b** molecule had C1 point group symmetry containing 24 atoms and a 66 base vibration frequency, the **2c** molecule had C1 point group symmetry and an 84 base vibration frequency. In addition, vibration frequencies were calculated with the DFT(B3LYP/6-31G(d)) basis set for all monomer and tetramer structures in this study. The calculated spectra are displayed in Fig. 5. In order to approximate the calculation results compared to the experimental results, each frequency value was multiplied with the scale value of 0.9613 [57]. It was observed that the experimental results were closer to vibration frequency values calculated for the tetramer structure (Fig. 6) when compared to the monomer structure.

The $-NH_2$ group is found in the compounds **2b** and **2c**. We can expect the $-NH_2$ group to have a symmetric vibration and also an asymmetric vibration. In the literature, theoretical $-NH_2$ symmetric and asymmetric vibration frequencies have been given as 3230–3150 and 3450–3300 cm^{-1}, respectively. In addition, the $-NH_2$ bending vibration frequency range has been reported as 1640–1580 cm^{-1} [58,59]. In the cases of N–H or O–H groups regarding molecules forming an intermolecular or intramolecular hydrogen bond, the stretching vibration frequency values of these groups decrease while their bending vibration frequency values increase [60].

Theoretically, the $-NH_2$ asymmetric vibration frequency was

Table 3
Intermolecular interaction geometries for $C_9H_8N_4O_2S$ (**2b**) and $C_{11}H_{13}N_3O_2S$ (**2c**) single crystals (Å, °).

	D-H	H···A	D···A	D-H···A
$C_9H_8N_4O_2S$ (2b)				
N1– H1···N2^{i}				
Experimental	0.86(3)	2.18(3)	3.047(3)	176(3)
DFT	1.03	1.94	2.97	175
N1– H2···N2^{ii}				
Experimental	0.85(4)	2.53(4)	3.332(3)	159(3)
DFT	1.02	2.11	3.00	144
C5–H5···Cg1^{iii}				
Experimental	0.93(3)	2.63(3)	3.47(3)	154(3)
Symmetry codes:i = −x+3,−y, z, **ii** = x, y+1, z, **iii** = −1+x,y,z				
$C_{11}H_{13}N_3O_2S$ (2c)				
N1B–H1B···N2A^{iv}				
Experimental	0.86(4)	2.18(4)	3.019(4)	167(4)
DFT	1.02	1.94	2.96	170
N1B–H2B···N3B^{v}				
Experimental	0.86(3)	2.10(3)	2.94(3)	167(3)
DFT	1.02	2.05	3.04	163
N1A-H1A···N2B^{vi}				
Experimental	0.86(4)	2.11(4)	2.96(4)	171(4)
DFT	1.03	1.97	3.00	172
N1A-H2A···N3A^{vii}				
Experimental	0.86(3)	2.25(3)	3.03(3)	151(3)
DFT	1.02	2.03	3.04	167
Symmetry codes:iv = x,−1+y,z, **v** = x,3/2-y,1/2 + z, **vi** = x,1 + y,z, **vii** = x,5/2-y,-1/2 + z				

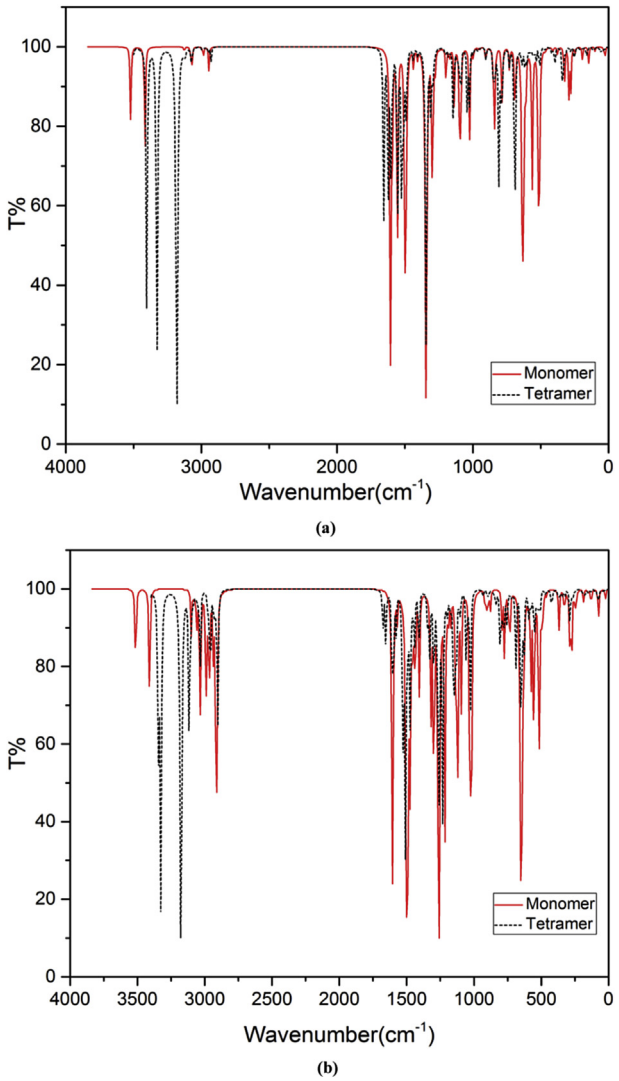

Fig. 5. Theoretical IR spectra of (a) **2b**, (b) **2c** compounds.

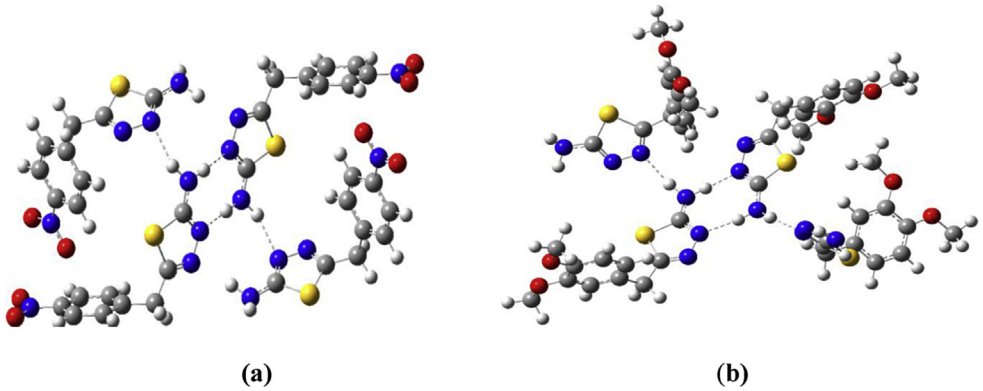

Fig. 6. Optimized tetramer structures calculated for (a) **2b**, (b) **2c** compounds.

calculated as 3403 cm^{-1} and 3345 cm^{-1} for the tetramer structures of **2b** and **2c** molecules, while it was calculated as 3627 cm^{-1} and 3513 cm^{-1} for the monomer structures of **2b** and **2c** molecules, respectively. Similarly, the $-NH_2$ symmetric vibration frequency was calculated as 3141 cm^{-1} and 3176 cm^{-1} for tetramer structures of **2b** and **2c** molecules, while it was calculated as 3349 cm^{-1} and 3410 cm^{-1} for monomer structures of **2b** and **2c** molecules, respectively. Experimentally, $-NH_2$ asymmetric vibration frequency was observed to be 3271 cm^{-1} and 3267 cm^{-1} for **2b** and **2c** compounds respectively, $-NH_2$ symmetric vibration frequency was observed to be 3112 cm^{-1} and 3083 cm^{-1} for **2b** and **2c** compounds, respectively.

In addition, the angle bending vibration frequency was calculated as 1662 cm^{-1} and 1675 cm^{-1} for tetramer structures of **2b** and **2c** molecules, while it was calculated as 1622 cm^{-1} and 1605 cm^{-1} for monomer structures of **2b** and **2c** compounds, respectively. Experimentally, this value was observed to be 1602 cm^{-1} and 1629 cm^{-1} for **2b** and **2c** compounds, respectively. In the light of these results, it can be concluded that the $-NH_2$ group can be used for intermolecular bonds.

Theoretically, stretching vibration frequency of monomer structures belonging to C=N, N–N and C–S groups in the thiadiazole ring was calculated to be 1501/1490, 1137 and 639/609 cm^{-1}, respectively for **2b** compound, whereas it was calculated to be 1503/1491, 1139 and 632/578 cm^{-1}, respectively for **2c** compound. These values were stated to be 1550/1490, 1141 and 726/561 cm^{-1} in the literature [61].

Experimentally, stretching vibration frequency of C=N group in the thiadiazole ring was observed to be 1531/1506 cm^{-1} and 1589/1511 cm^{-1} for **2b** and **2c** compounds, respectively. N–N stretching vibration frequency was observed to be 1155/1135 cm^{-1} for **2b** and **2c** compounds respectively, whereas C–S stretching vibration frequency was observed to be 622/603 cm^{-1} and 633/577 cm^{-1} for **2b** and **2c** compounds respectively. It was observed that the experimental measurements and theoretical calculations were compatible with the values found in the literature [62–66].

4.3. ^{1}H and ^{13}C NMR spectra (compounds **2b** and **2c**)

The GIAO (Gauge-Independent Atomic Orbital) method [67,68] was used to determine NMR chemical shift values of the molecules (**2b** and **2c**) and TMS (tetramethylsilane) was taken as reference. Dimethyl sulfoxide (DMSO) solvent was used for TMS and ^{1}H NMR, and ^{13}C NMR chemical shift values calculated for DFT/B3LYP/

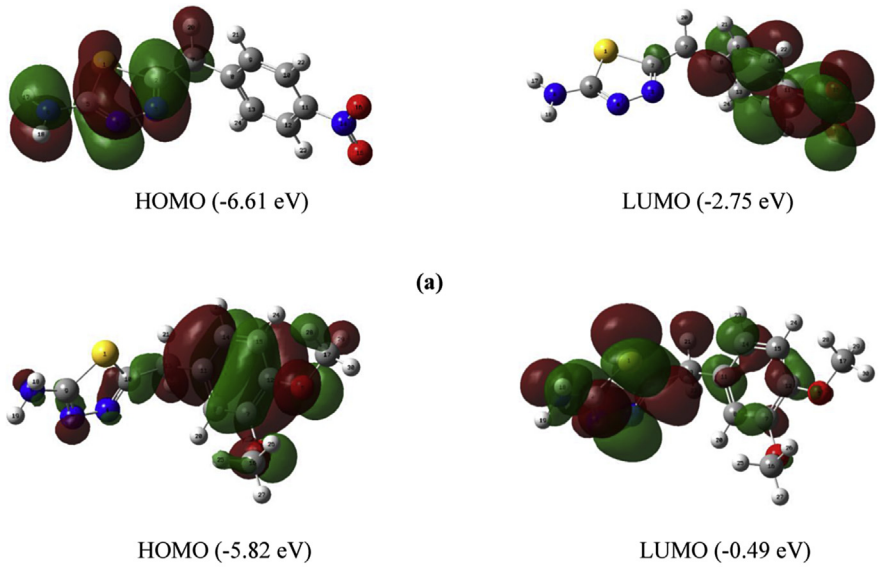

Fig. 7. Frontier orbitals and energies of (a) **2b**, (b) **2c** compounds.

6-31G(d) were 32.1 and 189.4 ppm, respectively. ^{1}H NMR and ^{13}C NMR chemical shift values for **2b** and **2c** compounds obtained theoretically using experimental and optimized structures are given in Table S1. (Table S1 is provided as Supplementary Material). As can be seen in the ^{13}C NMR spectrum of molecules (**2b** and **2c**), the peaks of C1 and C2 atoms constitute evidence that the compounds have a thiadiazole ring. Chemical shift values of these atoms were higher than other carbon atoms. Three electronegative atoms (N1, N2, and S1) around the C1 atoms especially resonate in the low field due to the high deshielding effect of these atoms, and this causes the chemical shift values of **2b** and **2c** atoms to be 168.3 ppm and 166.6 ppm, respectively, which are higher when compared to other carbon atoms.

Experimentally, chemical shifting value of C1 atom was found to be 169.8 ppm and 169.5 ppm for **2b** and **2c** compounds, respectively.

Theoretically, C2 atoms found in **2b** and **2c** molecules (together with two N3 and S1 atoms) had lower electronegativity when compared to the N1 atom, and they therefore resonated in a higher field due to the lower deshielding effect. This occurrence caused chemical shift values to be 164.8 ppm for the **2b** molecule and 161.6 ppm for the **2c** molecule, which is comparatively lower.

Experimentally, chemical shifting value of C2 atom was found to be 156.4 ppm and 159.0 ppm for **2b** and **2c** compounds, respectively. It was observed that the experimental measurements and theoretical calculations were compatible with the values found in the literature [66–69].

In the ^{1}H NMR spectra, the hydrogen peak belonging to the $-NH_2$ groups were observed at 7.1 ppm and 7.0 ppm corresponding to two protons for compounds **2b** and **2c**, respectively. In theoretical calculations, these peaks were found to be 4.4 ppm for the **2b** molecule and 3.7–4.0 ppm for the **2c** molecule which is almost the half the value of the experimental results. This result might be due to the assumption in the theoretical calculation that the molecule does not have the N–H … N hydrogen bond. Other theoretical and experimental ^{13}C NMR and ^{1}H NMR peaks belonging to the compounds **2b** and **2c** are given in Table S1. (Table S1 is provided as Supplementary Material).

*4.4. Frontier molecular orbital analysis and molecular hardness parameters (compounds **2b** and **2c**)*

After stable structures and structural parameters for these molecules (**2b** and **2c**) were obtained, the following parameters were examined: induced dipole moment; polarizability; first hyperpolarizability; HOMO and LUMO energy values. At the same time, hardness was obtained from these energy values. In this study we investigated how these properties changed with the effects of different electron-providing groups.

The most important orbitals in molecules are frontier molecular orbitals called HOMO and LUMO. The energy difference between these orbitals is a measure of the chemical stability of the molecule. Since it is also a measure of electron conductivity, it is a critical parameter to determine the molecular electrical transport property. Therefore, this energy difference is largely responsible for chemical and spectroscopic properties of a molecule [70].

The calculations were made in the gas phase. For these molecules, the HOMO energy value was found to be −6.61 and −5.82 eV, while the LUMO energy value was found to be −2.75 and −0.49 eV, respectively. The difference between these energy levels ($\Delta E_{HOMO-LUMO}$) was 3.86 for **2b** and 5.33 for **2c**. In the examined molecules, it was seen that electron withdrawing groups and electron donating groups bonded to two phenyl rings and polarized the charge distribution. The dipole moment changed as a result.

As shown in Fig. 7, the electron donating $-OCH_3$ group localized the HOMO orbitals in the **2c** molecule while the electron withdrawing $-NO_2$ group bonded to phenyl ring localized the LUMO orbitals in the **2b** molecule.

Molecular hardness parameters were obtained using the finite difference formula suggested by Parr and Pearson [71,72], and they were calculated using the operational definition of the hardness parameter η:

$$\eta = 1/2\ (IE-EA)$$

Here, IE indicates the initial ionization energy and EA indicates the electron affinity. The hardness value can provide the following approach through the highest occupied molecular orbital energies

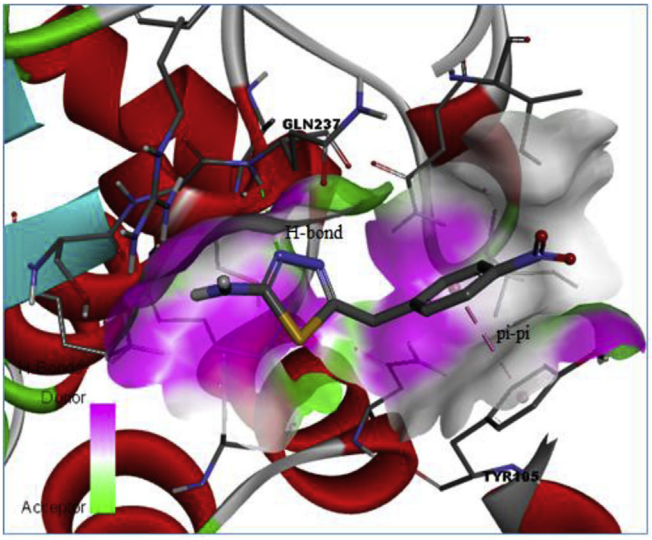

(a)

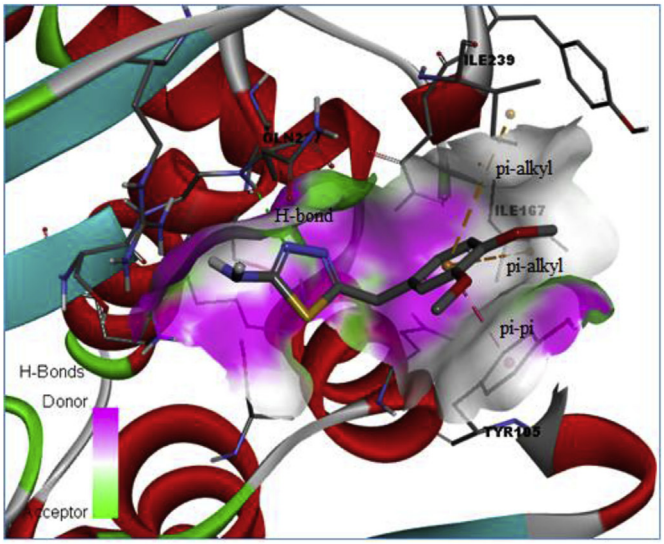

(b)

Fig. 8. Representation of docking results of (a) **2b**, (b) **2c** compounds. H-bond, π–π, and π-alkyl interactions are represented with green, pink, and orange lines, respectively. (For interpretation of the references to colour in this figure legend, the reader is referred to the web version of this article.)

Table 4
Affinity and RMSD values of different confirmations of **2b** and **2c** molecules.

Compound 2b				Compound 2c			
Mode	Affinity (kcal/mol)	Distance from best mode		Mode	Affinity (kcal/mol)	Distance from best mode	
		RMSD 1.b.	RMSD u.b.			RMSD 1.b.	RMSD u.b.
1	−6.7	0.000	0.000	**1**	−6.2	0.000	0.000
2	−6.5	4.516	6.831	**2**	−6.0	2.387	3.484
3	−6.4	3.847	4.880	**3**	−5.9	1.357	2.604
4	−6.3	2.719	3.500	**4**	−5.9	2.254	3.261
5	−6.2	4.397	5.972	**5**	−5.9	1.503	1.899
6	−6.2	1.483	1.812	**6**	−5.9	2.467	3.263
7	−5.9	1.771	1.864	**7**	−5.6	4.268	5.795
8	−5.8	3.826	4.983	**8**	−5.6	4.321	5.442
9	−5.5	2.448	3.136	**9**	−5.6	3.047	5.040

(E_{HOMO}) and the lowest unoccupied molecular orbital energies (E_{LUMO}):

$$\eta \approx 1/2(E_{LUMO} - E_{HOMO})$$

In some studies found in the literature, the effects of the hardness parameter η on charge transfers were examined, and it was reported in these studies that a small η value indicated a stronger charge transfer interaction [73–75]. The hardness value was calculated to be 3.86 and 5.33 for **2b** and **2c**, respectively. The fact that the hardness value calculated for the **2b** molecule was lower when compared to the **2c** molecule shows that the charge transfer will be stronger in the **2b** molecule.

4.5. Molecular docking studies (compounds **2b** and **2c**)

The Beta-Lactamase crystal structure (pdb code: 1BLH) for docking works was obtained from the Protein Data Bank (http://www.rcsb.org/pdb). Before the docking process, water molecules were removed from the Beta-Lactamase of *S. aureus* (PDB: 1BLH), and hydrogen atoms and Gasteiger charges were added. Ligands of **2b** and **2c** molecules were then docked to target molecule binding sites (Fig. 8). Autodock Vina [76] was used for docking works and AutoDock Tools was used for creating docking data entry files. Receptor-ligand interactions were demonstrated with Discover Studio Visualizer 4.0 and Pymol softwares. The estimated bonding energy as a result of molecular docking (docking score) and RMSD values are given comparatively in Table 4.

The docking results were accepted as correct when the RMSD value was lower than 2 Å [77]. The RMSD value is the root mean square deviation from the determined confirmation of the ligand structure. In other words, this value indicates the deviation of the ligand from the active site with which it interacts, and it is the most important criterion used for docking results. The criterion to be considered after RMSD is the bonding energy. The reason behind this priority order is that the structure may give low bonding energy outside the active site as well. Therefore, first the proximity to the active site is considered and then the energy of the bonding in the active site.

It was observed that the ligand bonded to substrate bonding sites of receptors with weak, non-covalent interactions, and more specifically hydrogen bonding with π-π and π-alkyl interactions. As seen in Fig. 8, a hydrogen bond of 2.304 Å occurred for the **2b** ligand and 2.297 Å occurred for the **2c** ligand between GLN237 and the N atom. As shown in Fig. 8, TYR105 bonded to the phenyl ring of the **2b** ligand with the π-π interaction, while ILE239 and ILE167 bonded to the phenyl ring of **2c** ligand with the π-alkyl interaction. According to the calculated bonding affinities, these initial results show that the **2b** and **2c** compounds might inhibit the Beta-Lactamase enzyme. Thus, new antibiotic agents may be developed. However biological tests need to be done so as to validate the computational predictions.

5. Conclusions

In this study, compounds containing 2-amino-1,3,4-thiadiazoles and their acyl derivatives were synthesized with high yields and with easily applicable methods. The structures of all synthesized compounds were elucidated with various spectroscopic methods.

Among the synthesized compounds, single-crystal versions of compounds **2b** and **2c** were obtained. After the stable structures and structural parameters of these compounds were calculated, their HOMO, LUMO energies and hardness parameters of these energies were found. The effects of electron donating groups ($-OCH_3$) and electron withdrawing groups ($-NO_2$) in these molecules (**2b** and **2c**) were investigated. The fact that the hardness value calculated for the **2b** molecule was lower compared to the **2c** molecule demonstrates that the charge transfer is stronger in the **2b** molecule. Finally, the docking simulation process was used to obtain possible bonding models and confirmations for **2b** and **2c** compounds. Docking study results show that the **2b** and **2c** compounds might inhibit the Beta-Lactamase enzyme, thus new antibiotic agents may be developed.

Acknowledgments

The financial support under the contract (KBÜ-BAP-14/1-YL-012) from the Karabük University is gratefully acknowledged. In addition, computing resources used in this work were provided by the National Center for High Performance Computing of Turkey (UHeM) under grant number 1002742013.

Appendix A. Supplementary data

Supplementary data related to this article can be found at http://dx.doi.org/10.1016/j.molstruc.2016.01.045.

References

[1] R.K. Dani, M.K. Bharty, S.K. Kushawaha, S. Paswan, O. Prakash, R.K. Singh, N.K. Singh, J. Mol. Struct. 1054 (2013) 251–261.
[2] H.S. Dong, B. Quan, D.W. Zhu, W.D. Li, J. Mol. Struct. 616 (2002) 1–5.
[3] J. Han, X.Y. Chang, Y.M. Wang, M.L. Pang, J.B. Meng, J. Mol. Struct. 937 (2009) 122–130.
[4] D.M. Egorov, Y.L. Piterskaya, A.V. Dogadina, N.I. Svintsitskaya, Tetrahedron Lett. 56 (2015) 1552–1554.
[5] N. Foroughifar, A. Mobinikhaledi, S. Ebrahimi, H. Moghanian, M.A.B. Fard, M. Kalhor, Tetrahedron Lett. 50 (2009) 836–839.
[6] J.P. Kilburn, J. Lau, R.C.F. Jones, Tetrahedron Lett. 44 (2003) 7825–7828.
[7] L. Strzemecka, Z.U. Lipkowska, J. Mol. Struct. 970 (2010) 1–13.
[8] A.K. Jain, S. Sharma, A. Vaidya, V. Ravichandran, R.K. Agrawal, Chem. Biol.

Drug. Des. 81 (2013) 557–576.
[9] N. Polkam, P. Rayam, J.S. Anireddy, S. Yennam, H.S. Anantaraju, S. Dharmarajan, Y. Perumal, S.S. Kotapalli, R. Ummanni, S. Balasubramanian, Bioorg. Med. Chem. Lett. 25 (2015) 1398–1402.
[10] M. Yoosefian, Z.J. Chermahini, H. Raissi, A. Mola, M. Sadeghi, J. Mol. Liq. 203 (2015) 137–142.
[11] T.A. Farghaly, M.A. Abdallah, G.S. Masaret, Z.A. Muhammad, Eur. J. Med. Chem. 97 (2015) 320–333.
[12] B. Chandrakantha, A.M. Isloor, P. Shetty, H.K. Fun, G. Hegde, Eur. J. Med. Chem. 71 (2014) 316–323.
[13] S. Chandra, S. Gautam, A. Kumar, M. Madan, Spectrochim. Acta A 136 (2015) 672–681.
[14] Y. Luo, S. Zhang, Z.J. Liu, W. Chen, J. Fu, Q.F. Zeng, H.L. Zhu, Eur. J. Med. Chem. 64 (2013) 54–61.
[15] M.F. El Shehry, A.A. Abu-Hashem, E.M. El-Telbani, Eur. J. Med. Chem. 45 (2010) 1906–1911.
[16] A.A. Kadi, E.S. Al-Abdullah, I.A. Shehata, E.E. Habib, T.M. Ibrahim, A.A. El-Emam, Eur. J. Med. Chem. 45 (2010) 5006–5011.
[17] J.J. Luszczki, M. Karpinska, J. Matysiak, A. Niewiadomy, Pharmacol. Rep. 67 (2015) 588–592.
[18] H.N. Dogan, A. Duran, S. Rollas, G. Sener, M.K. Uysal, D. Gülen, Bioorg. Med. Chem. 10 (2002) 2893–2898.
[19] P. Zhan, X. Liu, Z. Li, Z. Fang, Z. Li, D. Wang, C. Pannecouque, E. De Clercq, Bioorg. Med. Chem. 17 (2009) 5920–5927.
[20] A.R. Bhat, Tazeem, A. Azam, I. Choi, F. Athar, Eur. J. Med. Chem. 46 (2011) 3158–3166.
[21] S.N. Swamy, Basappa, B.S. Priya, B. Prabhuswamy, B.H. Doreswamy, J.S. Prasad, K.S. Rangappa, Eur. J. Med. Chem. 41 (2006) 531–538.
[22] S.F. Barbuceanu, G. Saramet, G.L. Almajan, C. Draghici, F. Barbuceanu, G. Bancescu, J. Med. Chem. 49 (2012) 417–423.
[23] N. Siddiqui, W. Ahsan, Med. Chem. Res. 20 (2011) 261–268.
[24] X.Q. Shen, H.J. Zhong, H. Zheng, H.Y. Zhang, G.H. Zhao, Q.A. Wu, H.Y. Mao, E.B. Wang, Y. Zhu, Polyhedron 23 (2004) 1851–1857.
[25] A.A. Kadi, N.R. El-Brollosy, O.A. Al-Deeb, E.E. Habib, T.M. Ibrahim, A.A. El-Emam, Eur. J. Med. Chem. 42 (2007) 235–242.
[26] S. Kumar, V. Gopalakrishnan, M. Hegde, V. Rana, S.S. Dhepe, S.A. Ramareddy, A. Leoni, A. Locatelli, R. Morigi, M. Rambaldi, M. Srivastava, S.C. Raghavan, S.S. Karki, Bioorg. Med. Chem. Lett. 24 (2014) 4682–4688.
[27] G. Revelant, C. Gadais, V. Mathieu, G. Kirsch, S. Hesse, Bioorg. Med. Chem. Lett. 24 (2014) 2724–2727.
[28] D. Kumar, N.M. Kumar, B. Noel, K. Shah, Eur. J. Med. Chem. 55 (2012) 432–438.
[29] K.M. Dawood, T.M.A. Eldebss, H.S.A. El-Zahabi, M.H. Yousef, P. Metz, Eur. J. Med. Chem. 70 (2013) 740–749.
[30] A. Husain, M. Rashid, R. Mishra, S. Parveen, D.S. Shin, D. Kumar, Bioorg. Med. Chem. Lett. 22 (2012) 5438–5444.
[31] W. Rzeski, J. Matysiak, M. Kandefer-Szerszen, Bioorg. Med. Chem. 15 (2007) 3201–3207.
[32] M.R. De Giorgi, R. Carpignano, A. Cerniani, Dyes Pigments 37 (1998) 187–196.
[33] M.C.R. Castro, P. Schellenberg, M. Belsley, A.M.C. Fonseca, S.S.M. Fernandes, M.M.M. Raposo, Dyes Pigments 95 (2012) 392–399.
[34] Y. Hu, C.Y. Li, X.M. Wang, Y.H. Yang, H.L. Zhu, Chem. Rev. 114 (2014) 5572–5610.
[35] G.G.R. Calero, S. Conte, M.A. Lowe, J. Gao, Y. Kiya, J.C. Henderson, H.D. Abruna, Electrochim. Acta 167 (2015) 55–60.
[36] P.A. Bradford, Clin. Microbiol. Rev. 14 (2001) 933–951.
[37] S.Y. Essack, Pharm. Res. 18 (2001) 1391–1399.
[38] Bruker. APEX2 and SAINT, Bruker AXS Inc., Madison, Wisconsin, USA, 2008.
[39] G.M. Sheldrick, Acta Cryst. C71 (2015) 3–8.
[40] L.J. Farrugia, J. Appl. Cryst. 45 (2012) 849–854.
[41] A.L. Spek, Acta. Cryst. D65 (2009) 148–155.
[42] C.F. Macrae, I.J. Bruno, J.A. Chisholm, P.R. Edgington, P. McCabe, E. Pidcock, L. Rodriguez-Monge, R. Taylor, J. van de Streek, P.A. Wood, J. Appl. Cryst. 41 (2008) 466–470.
[43] G. Rauhut, S. Puyear, K. Wolinski, P. Pulay, J. Phys. Chem. 100 (1996) 6310–6316.
[44] R. Ditchfield, W.J. Hehre, J.A. Pople, J. Chem. Phys. 54 (1971) 724–728.
[45] M.J. Frisch, G.W. Trucks, H.B. Schlegel, G.E. Scuseria, M.A. Robb, J.R. Cheeseman, Gaussian 09, Revision B.01, Gaussian, Inc., Wallingford CT, 2010.
[46] R. Dennington, T. Keith, J. Millam, GaussView, Version 5, Semichem Inc., Shawnee Mission KS, 2009.
[47] M. Er, Y. Ünver, K. Sancak, E. Dügdü, Arkivoc 15 (2008) 99–120.
[48] M. Er, Y. Ünver, K. Sancak, İ. Degirmencioğlu, Ş.A. Karaoglu, Arkivoc 2 (2009) 149–167.
[49] D.Y. Ra, N.S. Cho, J.J. Cho, J. Heterocycl. Chem. 35 (1998) 525–530.
[50] M. Er, A. Şahin, H. Tahtaci, Maced. J. Chem. Chem. Eng. 33 (2014) 189–198.
[51] K. Sancak, Y. Ünver, M. Er, Turk. J. Chem. 31 (2007) 125–134.
[52] J.P. Jasinski, M.K. Bharty, N.K. Singh, S.K. Kushawaha, R.J. Butcher, J. Chem. Crystallogr. 41 (2011) 6–11.
[53] F. Bentiss, M. Lagrenee, H. Vezin, J.P. Wignacourt, E.M. Holt, Polyhedron 23 (2004) 1903–1907.
[54] M.K. Bharty, A. Bharti, R.K. Dani, S.K. Kushawaha, R. Dulare, N.K. Singh, Polyhedron 41 (2012) 52–60.
[55] D. Glossman-Mitnik, A. Marquez-Lucero, J. Mol. Struct. (Theochem) 548 (2001) 153–163.
[56] M.F. Erben, C.O. Della Védova, R. Boese, H. Willner, C. Leibold, H. Oberhammer, Inorg. Chem. 42 (2003) 7297–7303.
[57] J.B. Foresman, in: E. Frisch (Ed.), Exploring Chemistry with Electronic Structure Methods, A Guide to Using Gaussian, Pittsburg, PA, 1996.
[58] R.M. Silverstein, G.C. Bassler, Spectrometric Identification of Organic Compounds, second ed., John Wiley and Sons Inc., New York, 1967.
[59] N.P.G. Roeges, A Guide to the Complete Interpretation of Infrared Spectra of Organic Structures, Wiley, New York, 1994.
[60] Ç. Yüksektepe, N. Çalışkan, İ. Yılmaz, A. Çukurovalı, J. Chem. Crystallogr. 40 (2010) 1049–1059.
[61] T.A. de Toledo, L.E. da Silva, A.M.R. Teixeira, P.T.C. Freire, P.S. Pizani, J. Mol. Struct. 1091 (2015) 37–42.
[62] A. Saeed, A. Khurshid, M. Bolte, A.C. Fantoni, M.F. Erben, Spectrochim. Acta A 143 (2015) 59–66.
[63] I.A. Shaaban, A.E. Hassan, A.M. Abuelela, W.M. Zoghaieb, T.A. Mohamed, J. Mol. Struct. 1103 (2016) 70–81.
[64] K. Gholivand, S. Farshadian, M.F. Erben, C.O. Della Védova, J. Mol. Struct. 978 (2010) 67–73.
[65] Y.I. Slyvka, E.A. Goreshnik, B.R. Ardan, G. Veryasov, D. Morozov, M.G. Mys'kiv, J. Mol. Struct. 1086 (2015) 125–130.
[66] P. Gautam, O. Prakash, R.K. Dani, N.K. Singh, R.K. Singh, Spectrochim. Acta A 132 (2014) 278–287.
[67] R. Ditchfield, J. Chem. Phys. 56 (1972) 5688–5691.
[68] K. Wolinski, J.F. Hinton, P. Pulay, J. Am. Chem. Soc. 112 (1990) 8251–8260.
[69] T.A. Mohamed, U.A. Soliman, I.A. Shaaban, W.M. Zoghaib, L.D. Wilson, Spectrochim. Acta A 150 (2015) 339–349.
[70] P.W. Atkins, Physical Chemistry, Oxford University Press, Oxford, 2001.
[71] R.G. Parr, R.G. Pearson, J. Am. Chem. Soc. 105 (1983) 7512–7516.
[72] A.K. Chandra, T. Uchimaru, Hardness profile: a critical study, J. Phys. Chem. A 105 (2001) 3578–3582.
[73] K. Mandal, T. Kar, P.K. Nandi, S.P. Bhattacharyya, Chem. Phys. Lett. 376 (2003) 116–124.
[74] P.K. Nandi, K. Mandal, T. Kar, Chem. Phys. Lett. 381 (2003) 230–238.
[75] P.K. Nandi, K. Mandal, T. Kar, J. Mol. Struct. (Theochem) 760 (2006) 235–244.
[76] O. Trott, A.J. Olson, J. Comput. Chem. 31 (2010) 455–461.
[77] B. Kramer, M. Rarey, T. Lengauer, Proteins Struct. Funct. Genet. 37 (1999) 228–241.